This is a pre-copyedited, author-produced version of an article accepted for publication in Light Metals 2021 following peer review. The final authenticated version is available online at https://doi.org/10.1007/978-3-030-65396-5_118.

Effect of ultrasonic melt treatment on the sump profile and microstructure of a direct-chill cast AA6008 aluminum alloy

Tungky Subroto[1,*], Gerard S. Bruno Lebon[1], Dmitry G. Eskin[1,2], Ivan Skalicky[3], Dan Roberts[3], Iakovos Tzanakis[4,5], and Koulis Pericleous[6]

[1]Brunel Centre for Advanced Solidification Technology (BCAST), Brunel University London, Uxbridge, UB8 3PH
[2]Tomsk State University, Tomsk, 634050, Russia
[3]Constellium UTC, Brunel University London, Uxbridge, UB8 3PH
[4]Faculty of Technology, Design and Environment, Oxford Brookes University, Oxford, OX33 1HX, UK
[5]Department of Materials, University of Oxford, Oxford, OX1 3PH, United Kingdom
[6]Computational Science and Engineering Group, University of Greenwich, 30 Park Row, London SE10 9LS, UK

[*] Corresponding author, E-mail address: Tungky.subroto@brunel.ac.uk

Abstract
This work focuses on the effects of ultrasonic melt treatment (UST) during direct-chill (DC) casting on the temperature distribution across the billet, sump profile and the resulting microstructure. Two AA6008 billets were cast; one was treated with UST in the hot top while the other was not. To determine the temperature distribution along the billet, multi-point temperature measurements were made across the radii of both billets. The sump profile was also analyzed through macrostructure analysis, after Zn was poured into the sump, while structure refinement was quantified through grain-size measurements. A numerical model of ultrasound-assisted DC casting is validated using the temperature measurements. As an outcome, this study provides information on the extent to which UST affects the sump profile and the corresponding changes in the microstructure. The knowledge gained from this study paves the way towards optimization of UST parameters in DC casting.

Keywords: Ultrasonic melt treatment, DC casting, aluminum alloy, temperature measurement, structure refinement.

1 Introduction

Direct-chill casting (DC-casting) is a semi-continuous casting process that is widely used by the industry to produce commercial aluminum alloy billets suitable for further rolling, extrusion or remelting processes [1]. Finer grain structure is typically required to avoid casting defects and improve technological properties of as-cast metal [2]. With increasing demands for better mechanical performance of aluminum alloys as postulated by the European Metallurgical Roadmap of 2050 different methods have been employed to achieve a refined microstructure with the addition of grain refiner being the most common practice used by industry [3]. To this end ultrasonic melt treatment (UST)is an alternative liquid metal treatment method which gains popularity and is becoming attractive for the industry as it is able to refine the structure of the cast product without the addition, or with significantly lesser amounts, of the environmental hazardous and expensive refiner agents [4]. UST utilizes the cavitation phenomenon, which is the result of high-frequency vibrations of the sonotrode tip within the melt. The structure refinement upon UST is attained through enhanced heterogeneous nucleation, by activation of dormant nuclei via wetting and mixing [5] (e.g. fragmented intermetallics and oxides) and dendrite fragmentation [4, 6] by the collapsing cavitation bubbles in the liquid melt [7]. In addition, the oscillating sonotrode generates a pressure wave in the melt that leads to the formation of macroscopic flow [8]. This flow, commonly termed ‘acoustic streaming’, is an important feature of UST as it extends ultrasonic activity to a larger melt volume [9].

When UST is performed in the hot top of a DC casting mold, the grain refinement effectiveness depends on the distance between the sonotrode and the solidification front [10]. Previous studies showed that the presence of forced convection in the vicinity of the solidification front may influence the structure [9, 11]. Therefore, it is important to understand the effect of sonotrode positioning in the DC casting in relation to the solidification front for optimization purposes.

Numerical modelling is a powerful tool used to obtain the optimum process parameters in DC casting of aluminum alloys [12]. An advanced numerical model of ultrasonic DC casting (UST-DC-casting) which includes the acoustic streaming phenomenon has been developed in an earlier study [13]. This model has been used to simulate UST-DC-casting with different UST parameters (i.e. sonotrode distance to solidification front and ultrasonic power) and the result could be logically explained through the grain structure analysis from the experiments [10]. However, the model has not been validated against the temperature profile from a DC casting experiment. This is important, as the temperature profile is directly linked to the sump shape and may affect the quality of the cast billet [11, 14], in addition to assessing the accuracy of the simulation.

In this work, we took temperature measurements using multiple thermocouples placed across the hot top on both conventional and UST-DC-castings. The results from the temperature measurements were then used to validate the numerical model ran using casting parameters matching the experiments. The sump shape and microstructure were also

analysed experimentally. The outcome of this study gives insight to the extent to which UST affects the sump profile and grain structure, critical factors towards the optimization of UST parameters in DC casting.

2 Methodology

2.1 Experimental

DC-casting of an AA6008 alloy was performed in the Advanced Metal Casting Centre (AMCC) of the Brunel Centre of Advanced Solidification Technology (BCAST) in Brunel University London. The billet had a diameter of 152 mm and was cast with a hot top. Two billets were cast at a casting speed of 140 mm min^{-1}; one billet was cast using conventional DC-casting, and another billet was cast with UST in the hot top. The billets were cast at a temperature of 668 ± 5 ºC. The experimental setup of the USP-DC casting is illustrated in Fig. 1(a). UST was carried out with a water-cooled 5-kW magnetostrictive transducer (Reltec) with a driving frequency of 17.3 kHz at a working power of 3.5 kW (which corresponds to 40 µm peak-to-peak amplitude). A conical Nb sonotrode with a working diameter of 20 mm was used to deliver ultrasonic power to the melt. The sonotrode tip was positioned approximately 20 mm above the graphite ring level/bottom part of the hot top.

Temperature distributions across the billet during both conventional and UST-DC-casting were measured using 5 type-K thermocouples with positions of each thermocouple as shown in Fig. 1(b). The positions of the thermocouples were selected to assess the effect of three-dimensional flow on the temperature profile across the billet during casting. Thermocouples were lowered with the casting speed when the casting had reached steady state.

Visualization of the sump profiles of both casts was done by pouring pure Zn melt into the melt pool. To enhance the contrast and obtain a better picture of the sump, the section of the billet with Zn was cut, mechanically polished and then etched using NaOH. Meanwhile, the effect of UST on microstructure was also verified through grain size analysis. For microstructure observation, samples were cut from different parts across the billet, from the center to the surface. The samples were ground and polished, then they were anodized in 5 wt.% HBF4 using 20 VDC, and subsequently examined under an optical microscope with polarized light. The grain size was measured using the linear intercept method taken randomly on optical microscope images and statistical analysis was performed.

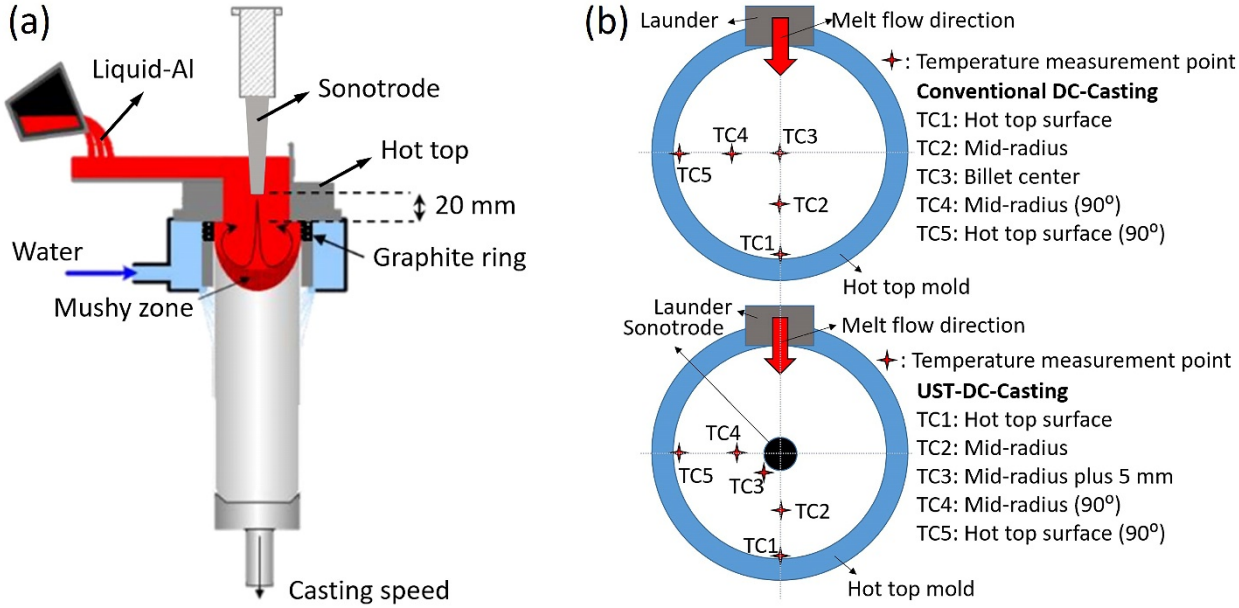

Fig. 1 (a) Illustration of UST-DC-casting setup with ultrasonic sonotrode positioned in the hot top (adapted from [10]), and (b) top-view of thermocouple positions across the hot top on both conventional DC-casting and UST-DC-casting.

2.2 Numerical

In parallel, a novel DC casting numerical model that considers the acoustic streaming phenomenon has been developed using OpenFOAM 6. The details of the model can be found elsewhere [13]. Simulations of both conventional and UST-DC-Casting cases were run with casting and UST parameters described in Section 2.1. The temperature profiles obtained from these simulations were then validated against thermocouple measurements taken at different points across the billet.

3 Result and discussion

The temperature recordings using thermocouples during DC-casting were used to validate the sump profiles obtained numerically as shown in Fig. 2. Good correlation was obtained for both conventional DC-casting and UST-DC-casting. This is shown by the position of the thermocouples at solid fraction of 0.7 or T = 641 ºC (yellow dots for conventional

DC-casting (left) and green dots for UST-DC-casting (right) in Fig. 2) correlates relatively well with the temperature profile distribution from numerical simulation results. In addition, the numerical model shows that the three-dimensional melt flow seems to provide symmetric temperature profile across the billet which is confirmed by the temperature recording from multiple-thermocouple measurements. The temperature profiles from numerical simulation results show that the liquidus isotherm of the UST-DC-Casting (Fig. 2 – right) is rather depressed as compared to the conventional DC casting (Fig. 2 – left) which is understandable as the acoustic streaming sends fresh supply of hot melt from the hot top towards the sump. This phenomenon was also observed in our previous work [13]. The flow pattern in Fig. 2 depicts that convection flow dominates in the conventional DC casting (blue arrow in Fig. 2 – left), which is a typical feature in a normal DC casting [14]. Convection flow is also present in the UST-DC-casting (the flow follows light blue arrow on Fig. 2 – right), however, this flow is opposed by the acoustic flow which the velocity has a magnitude much stronger than the convection flow (blue arrow in Fig. 2 – right) evidenced by the difference in the scaling of flow velocity in the UST-DC-casting plot. The difference in flow velocity magnitude between these two cases is shown by the flow velocity scale in Fig. 2.

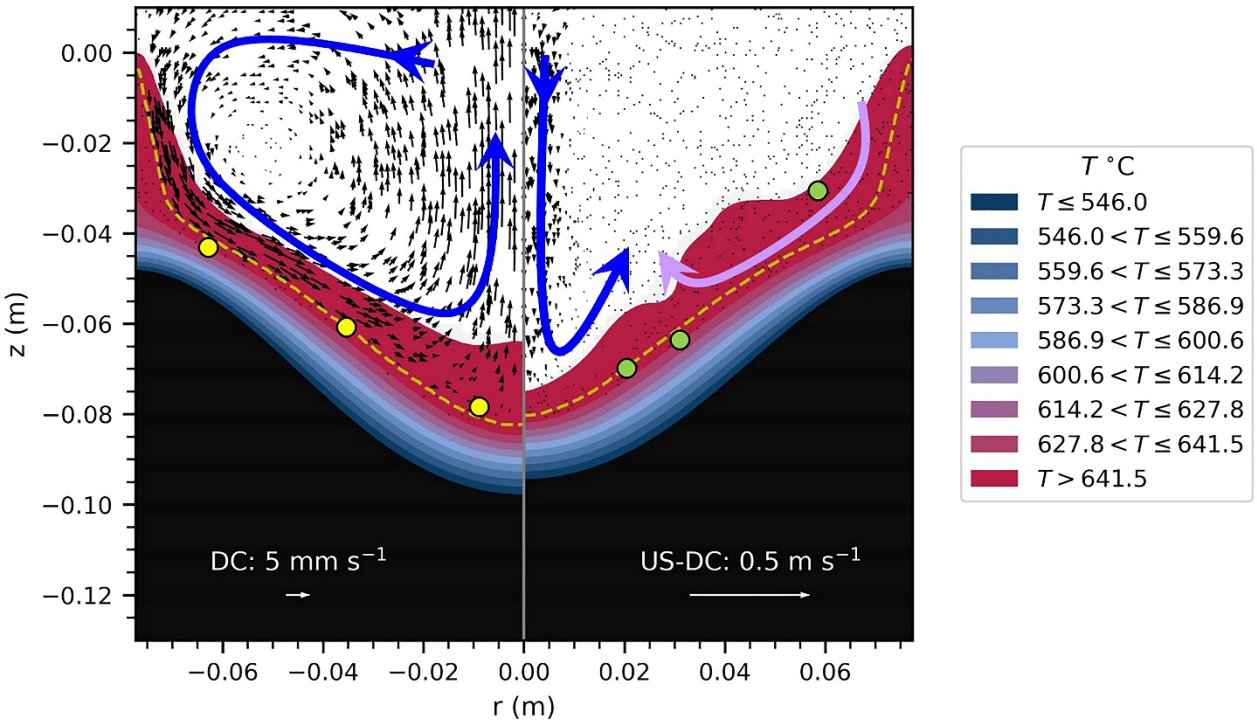

Fig. 2 Comparison of temperature profile and flow pattern from conventional DC-casting (left) and UST-DC-casting (right) simulations that have been validated with temperature measurement results. The dashed line illustrates isotherms at solid fraction of 0.7 (T = 641 ºC). Yellow dots in conventional DC-casting and green dots in UST-DC-casting result represent approximate position of the thermocouples at solid fraction of 0.7 (T = 641 ºC). Blue lines with arrows indicate the flow direction and patterns of the melt.

The sump profile visualization by Zn tracing shows that the conventional DC-casting produced marginally shallower sump profile and angle (Fig. 3(a)) as compared to the UST-DC-casting (Fig. 3(b)). Note that the observed profile does not represent the solidus isotherm. This is because Zn penetration could not go deeper into the fixed solid network (when dendrite coherency has been achieved or solid fraction is around 0.35-0.5) as only inter-dendritic feeding is possible in the mushy zone [15]. Therefore, the observed Zn profiles represent an isotherm at a rather lower solid fraction than the solidus. In the UST-DC-casting however, the presence of acoustic streaming may push Zn deeper into the mushy zone, thus exaggerating the observed sump depth in the UST-DC-casting. This suggests the presence of acoustic streaming when the sonotrode was positioned 20 mm above the graphite ring mostly affects the liquidus isotherm but only slightly modifies the position of the macroscopic solidification front (around the coherency isotherm). Although the Zn tracer visualization does not show sudden depression in the transition zone as shown by the numerical result, the result of temperature recording (green dots in Fig. 2) fairly capture the sudden depression in the UST-DC-casting case. This is understandable because it has been reported that the usage of higher density element (e.g. Zn and Cu) as tracer is convenient for sump visualization. Moreover, there is only short time available for Zn to dissolve in the melt and form an alloy. Thus, we expect minimum effect from the depressed solidus with Zn addition on the macroscopic profile. However, the result of temperature profiling using thermocouples is reported to have better accuracy [15].

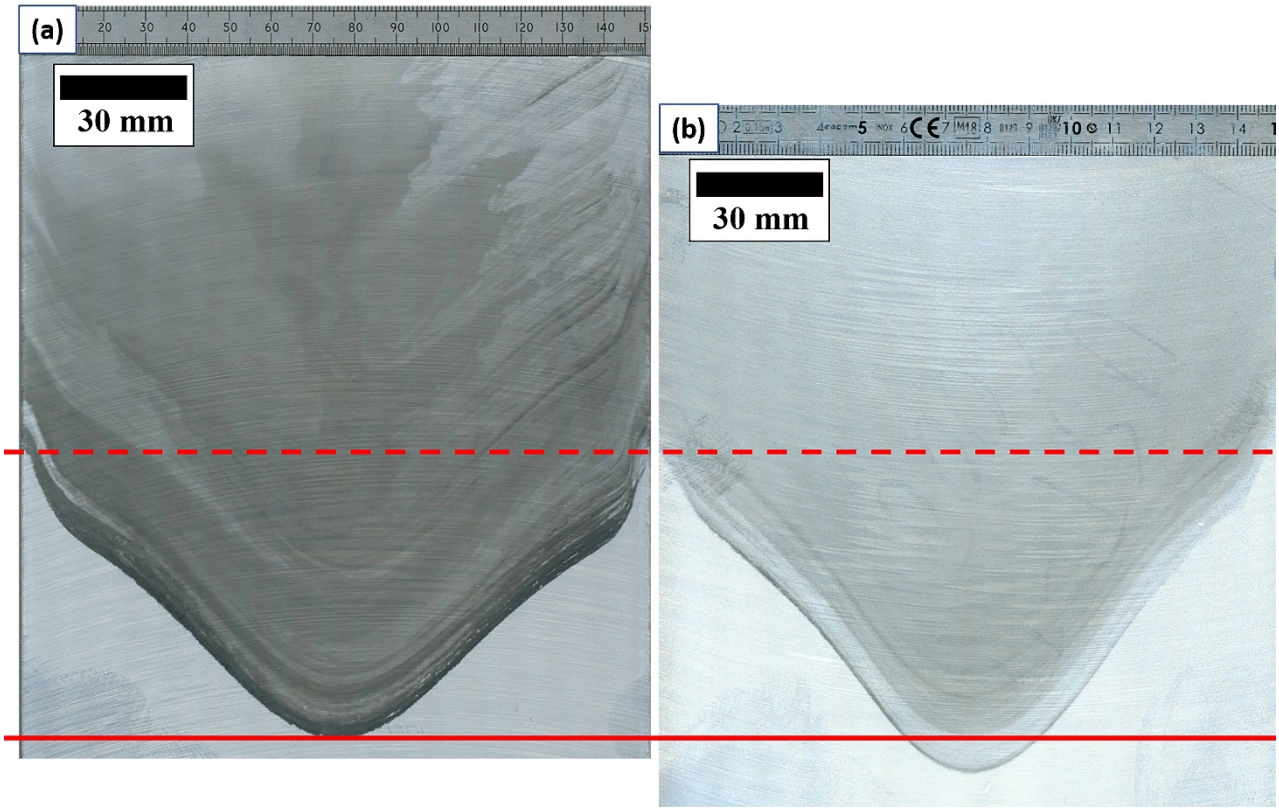

Fig. 3 Sump profiles (Zn-outlined) in the billets produced by (a) conventional DC casting and (b) UST-DC casting. Dashed line is used to compare the height where the shell starts to solidify for both billets, while solid line represents the maximum depth of Zn tracer penetration on conventional DC casting billet.

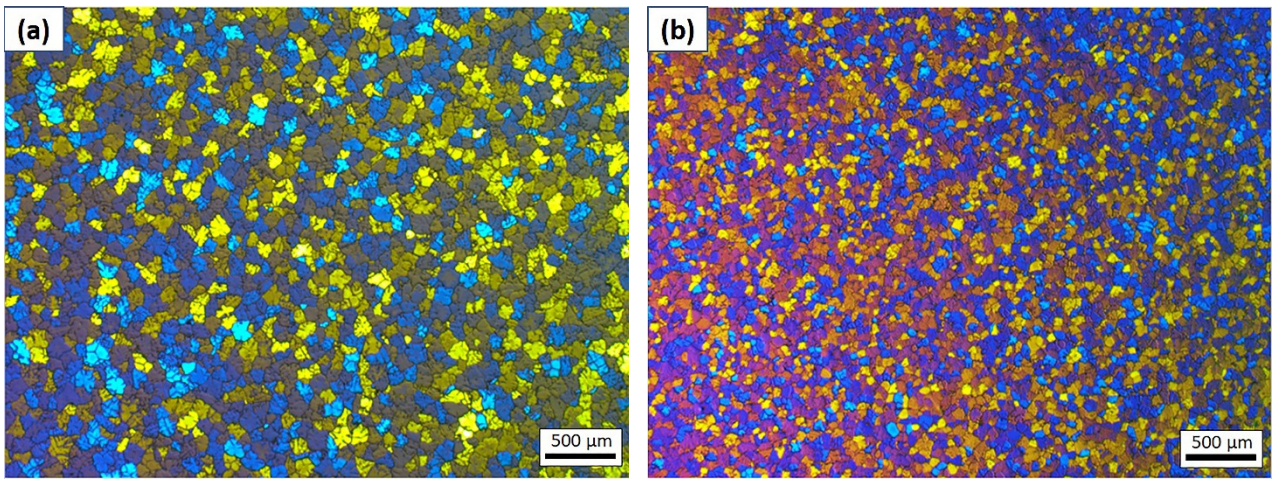

Fig. 4 Typical anodized grain structure in the center of the billet cast with (a) conventional DC-casting and (b) with UST-DC-casting.

The grain structure observation shown in Fig. 4 confirms the effectiveness of UST. The application of UST (Fig. 4(b)) in the hot top yields an approximately 50% size refinement in the center of the billet as compared to the conventional DC-casting (Fig. 4(a)). The average grain size of conventional DC casting in the center of the billet is around 100 µm while the UST-DC-casting is approximately 50 µm. In the conventional DC-casting, the grain structure coarsens from the surface to the center of the billet. On the contrary, in the UST-DC casting billet the finest grain structure was found in the billet center and it becomes a little coarser towards the surface of the billet. This could be explained by the proximity of the center of the billet to the active ultrasonic-treatment zone (both cavitation and acoustic streaming), which causes a narrower transition zone, more solidification centers and dendrite fragments (see Fig. 2(b)). While, the influence of UST decreases towards the billet surface as it is the furthermost from the cavitation zone.

The results obtained from this work, both the temperature measurements through thermocouples and visualization of the sump profile through Zn tracing, confirm the validity of the developed numerical model. Grain structure analysis also verifies the effectiveness of the UST in this experiment. This suggests that our model is a suitable step towards UST-DC-casting process optimization.

4 Conclusion

Multiple-thermocouples measurements have been carried out during both conventional and UST-DC-casting. The recorded temperature data were then used to validate the sump profile obtained by the developed UST-DC-casting simulation. The comparison yields good correlation between the measurement and the simulation result. Numerical simulation results show that UST application in the hot top with sonotrode position at 20 mm above the graphite ring level depresses the liquidus isotherm but does not affect much the solidus isotherm, resulting in a thinner transition region as compared to conventional DC-casting. Sump profile visualization through Zn tracer shows that UST-DC-casting produces steeper and marginally deeper sump profile as compared to the conventional DC-casting. However, such an occurrence may be due to acoustic streaming forcing the Zn to penetrate deeper into the mush. Grain structure analysis verifies that structure refinement has been achieved at the given sonotrode position. Strongest grain refinement effect was found in the center of the billet with grain size around 50% smaller than upon casting without UST.

Acknowledgements

Financial support from EPSRC (UK) under projects UltraMelt2 (EP/R011001/1, EP/R011044/1 and EP/R011095/1) and Future LiME Hub (EP/N007638/1) is gratefully acknowledged. The authors are thankful for the support of Constellium in running DC casting experiments in the AMCC/BCAST and Dr. N. Barekar for his help on macrostructure sample preparation.

References

1. Granger DA (1989) Ingot casting in the aluminum industry. In: Treatise on Materials Science & Technology. Elsevier, pp 109–135
2. Grandfield JF, Eskin DG, Bainbridge IF (2013) Direct-Chill Casting of Light Alloys: Science and Technology. John Wiley & Sons, Inc., Hoboken, NJ, USA
3. Murty BS, Kori SA, Chakraborty M (2002) Grain refinement of aluminium and its alloys by heterogeneous nucleation and alloying. International Materials Reviews 47:3–29. https://doi.org/10.1179/095066001225001049
4. Eskin GI, Eskin DG (2015) Ultrasonic Treatment of Light Alloy Melts, 2nd ed. CRC Press
5. Tzanakis I, Xu WW, Eskin DG, et al (2015) In situ observation and analysis of ultrasonic capillary effect in molten aluminium. Ultrasonics Sonochemistry 27:72–80. https://doi.org/10.1016/j.ultsonch.2015.04.029
6. Han Q (2015) Ultrasonic Processing of Materials. Metall and Materi Trans B 46:1603–1614. https://doi.org/10.1007/s11663-014-0266-x
7. Tzanakis I, Xu WW, Lebon GSB, et al (2015) In Situ Synchrotron Radiography and Spectrum Analysis of Transient Cavitation Bubbles in Molten Aluminium Alloy. Physics Procedia 70:841–845. https://doi.org/10.1016/j.phpro.2015.08.172
8. Lebon GSB, Tzanakis I, Pericleous K, et al (2019) Ultrasonic liquid metal processing: The essential role of cavitation bubbles in controlling acoustic streaming. Ultrasonics Sonochemistry 55:243–255. https://doi.org/10.1016/j.ultsonch.2019.01.021
9. Eskin DG, Jafari A, Katgerman L (2011) Contribution of forced centreline convection during direct chill casting of round billets to macrosegregation and structure of binary Al–Cu aluminium alloy. Materials Science and Technology 27:890–896. https://doi.org/10.1179/026708309X12578491814672
10. Salloum-Abou-Jaoude G, Eskin DG, Lebon GSB, et al (2019) Altering the Microstructure Morphology by Ultrasound Melt Processing During 6XXX Aluminium DC-Casting. In: Chesonis C (ed) Light Metals 2019. Springer International Publishing, Cham, pp 1605–1610
11. Zhang L, Eskin DG, Miroux A, et al (2012) Effect of inlet geometry on macrosegregation during the direct chill casting of 7050 alloy billets: experiments and computer modelling. IOP Conf Ser: Mater Sci Eng 33:012019. https://doi.org/10.1088/1757-899X/33/1/012019
12. Subroto T, Miroux A, Mortensen D, et al (2012) Semi-quantitative predictions of hot tearing and cold cracking in aluminum DC casting using numerical process simulator. IOP Conf Ser: Mater Sci Eng 33:012068. https://doi.org/10.1088/1757-899X/33/1/012068
13. Lebon GSB, Salloum-Abou-Jaoude G, Eskin D, et al (2019) Numerical modelling of acoustic streaming during the ultrasonic melt treatment of direct-chill (DC) casting. Ultrasonics Sonochemistry 54:171–182. https://doi.org/10.1016/j.ultsonch.2019.02.002
14. Nadella R, Eskin DG, Du Q, Katgerman L (2008) Macrosegregation in direct-chill casting of aluminium alloys. Progress in Materials Science 53:421–480. https://doi.org/10.1016/j.pmatsci.2007.10.001
15. Yu KC, Guo SJ, Nagaumi H (2016) Evaluation on the Accuracies of Sump Depth Measurements during DC Casting Process of 7050 Alloy. MSF 877:78–83. https://doi.org/10.4028/www.scientific.net/MSF.877.78